Potential Metallopharmaceutical agents; synthesis, spectroscopic characterization and antiproliferative study of novel metal complexes of tetra thiosemicarbazon ligand

Abdou S. El-Tabl[*1], Moshira M. Abd-El Wahed[2], Prasad V.Bharatam[3], Abdelhaleam A. Aly[1]

[1]Department of Chemistry, Faculty of Science, El-Menoufia University, Shebin El -Kom, Egypt.

[2]Department of Pathology, Faculty of Medicine, El-Menoufia University, Shebin El-Kom, Egypt.

[3] Department of Medicinal Chemistry, Natl. Inst.Pham.Edu.Res.(NIPER), S.A.S- Nagar-

Abstract: There has been much interesting in the development a new tetrathiosemicarbazone ligand and its Fe(III), Co(II), Ni(II), Cu(II), Zn(II), Cd(II), Pb(II), Al(III), Ca(II), Ba(II), Sr(II), Mg(II), and Ag(I), complexes . Complexes have been characterized by elemental analysis, IR, UV-Vis spectra , ^{1}H-NMR spectra, Mass spectra, Magnetic moments, Conductances, Thermal analyses (DTA and TGA) and ESR measurements The spectral data show that the ligand behaves a neutral or dibasic –octadentate type. Molar conductances in DMF solution indicate non-electrolytic nature of the prepared complexes. The ESR spectra of the solid complexes indicate anisotropic or isotropic type (dx^2-y^2) ground state with considerable covalent bond character. To study the cytotoxicity of the ligand and some of its metal complexes against human liver cancer cell (HePG-2 cell line). The cells were dosed with the complexes at varying concentrations and cell viability was measured by sulfo-rhodamine-B stain (SRB) method. The compounds show marked antiproliferative effect compared with a standard drug (vinblastine).

Keywords: thiosemicarbazone ligand, complexes, spectra, magnetism, antiproliferative study.

1 INTRODUCTION

Recently considerable attention have been given to thiosemicarbazones complexes due to not only for coordination chemistry but for pharmacological as well, due to their good complexes properties and significant biological activity [1,2]. Chemistry of transition metal complexes of thiosemicarbazones became largely appealing because of their broad profile of pharmacological activity that provides a diverse variety of compounds with different activities[3]. Some of the detected biological activities of the thiosemicarbazones and their complexes with transition metal ions are antibacterial, antifungal, antiarthritic, antimalarial, antitumor, antiviral and anti-HIV activities[4-6]. Thiosemicarbazone derivatives containing a 4-acyl-2-pyrazolin-5- one moiety form an important class of organic compounds due to their structural chemistry and biological activities[7,8]. In the field of anticancer research, the pyrazolones exhibited promising antiproliferative activity against human myelogenous leukaemia HL-606. The coordinating property of the 4-amino-2,3-dimethyl-1-phenyl-3-pyrazolin-5-one ligand has been modified to give a flexible ligand system, formed by condensation with a variety of reagents such as aldehydes, ketones[9-11], thiosemicarbazides and carbazides[12-14]. The biological properties of thiosemicarbazones are often related and modulated by metal ion coordination[15-17]. Cu (II), Ni (II) and Co (II) complexes of Schiff bases derived from 4, 6-diacetylresorcinol had been prepared and spectroscopically characterized[18].. Owing to the presence of the –NH-C=S functional group, thiosemicarbazones exhibit thion ethiol tautomerism and can bind to the metal ion either in the anionic thiolate form or in the neutral thione form. Generally thiosemicarbazones coordinate as bidentate ligand via azomethine nitrogen and thione/thiolate sulfur [19-21]. Physicochemical data of 6-(3-thienyl) pyridine-2-carboxaldehyde-4N-ethyl thiosemicarbazone, and 6-(3-thienyl) Pyridine-2-carboxaldehyde-4N-phenylthiosemicarbazone had been reported[22].Extensive investigation of metal complexes of thiosemicarbazones have been undertaken during the past several 56 years[23-26] . Here, we report the synthesis, structure, spectral, magnatic, and biological properties of (1Z,6Z)-diethylN'1,N'6-dicarbamothioyl-2-((E)-1-(2-carbamothioylhydrazono)ethyl)-5-((Z)1(2carbamothioylhydrazono)ethyl)hexanebis(hydrazonate) (H_4L)

2 MATERIALS AND METHODS

All the reagents employed for the preparation of the ligand and its complexes were synthetic grade and used without further puri-

fication. TLC is used to confirm the purity of the compounds. C, H, N and Cl analyses were determined at the Analytical Unit of Cairo University, Egypt. A standard gravimetric method was used to determine metal ions. All metal complexes were dried under vacuum over P_4O_{10}. The IR spectra were measured as KBr pellets using a Perkin-Elmer 683 spectrophotometer (4000-400 cm^{-1}). Electronic spectra (qualitative) were recorded on a Perkin-Elmer 550 spectrophotometer. The conductances(10^{-3}M) of the complexes in DMF were measured at 25 °C with a Bibby conduct meter type MCl. ^{1}H-NMR spectra of the ligand and its Cd(II) complex were obtained with Perkin-Elmer R32-90-MHz spectrophotometer using TMS as internal standard. Mass spectra were recorded using JEULJMS-AX-500 mass spectrometer provided with data sys-tem. The thermal analyses (DTA and TGA) were carried out in air on a Shimadzu DT-30 thermal analyzer from 27 to 800 °C at a heating rate of 10 °C per minute. Magnetic susceptibilities were measured at 25 °C by the Gouy method using mercuric tetrathiocyanatocobalt(II) as the magnetic susceptibility standard. Diamagnetic corrections were estimated from Pascal's constant. The magnetic moments were calculated from the equation: The ESR spectra of solid complexes at room temperature were recorded using a varian E-109 spectrophotometer, DPPH was used as a standard material.

2.1 PREPARATION OF THE LIGAND

2.1.1 PREPARATION OF 3-((2-AMINOPHENYL)AMINO)-3,4-DIHYDROQUINOXALIN-2(1H)-ONE:

Preparation of diethyl 2,5-diacetylhexanedioate: diethyl 2,5-diacetylhexanedioate (Scheme 1) was prepared by adding equimolar amount of dibromoethane (23.8 ml, 1 mol), to ethylacetoacetate (47.8 g, 2 mol) in 50 cm3 of absolute ethanol. The mixture was refluxed on water bath for one hour and then left to cool at room temperature, filtered off, washed with water, dried and recrystallized from ethanol to afford diethyl 2,5-diacetylhexanedioate.

2.1.2 PREPARATION OF THE SCHIFF-BASE LIGAND (1Z,6Z)-diethylN'1,N'6-dicarbamothioyl-2-((E)-1-(2-carbamothioylhydrazono)ethyl)-5-((Z)-1-(2carbamothioylhydrazono)ethyl)hexanebis(hydrazonate)(H_4L):

1Z,6Z)diethylN'1,N'6dicarbamothioyl2((E)1(2carbamothioylhydrazono)ethyl)-5-((Z)-1-(2carbamothioylhydrazono)ethyl)hexanebis(hydrazonate) (Scheme 1) was prepared by adding equimolar amount of diethyl 2,5-diacetylhexanedioate (28.6 g, 1 mol) to thiosemicarbazide (8.2 g, 4 mol) in 50 cm^3 of absolute ethanol. (thiosemicarbazide was dissolved in absolute ethanol contain drops of concentrated hydrochloric acid (HCl)) The mixture was refluxed with stirring for 3 hours. The white product which formed was filtrated off and washed with water, dried in air to give crude product. Then it was recrystallized from ethanol to give a pure needle shaped crystals of (1Z,6Z)-diethyl N'1,N'6-dicarbamothioyl-2-((E)-1-(2-carbamothioylhydrazno)ethyl)5((Z)1(2carbamothioylhydrazono)ethy l)hexanebis(hydrazonate) (H_4L)

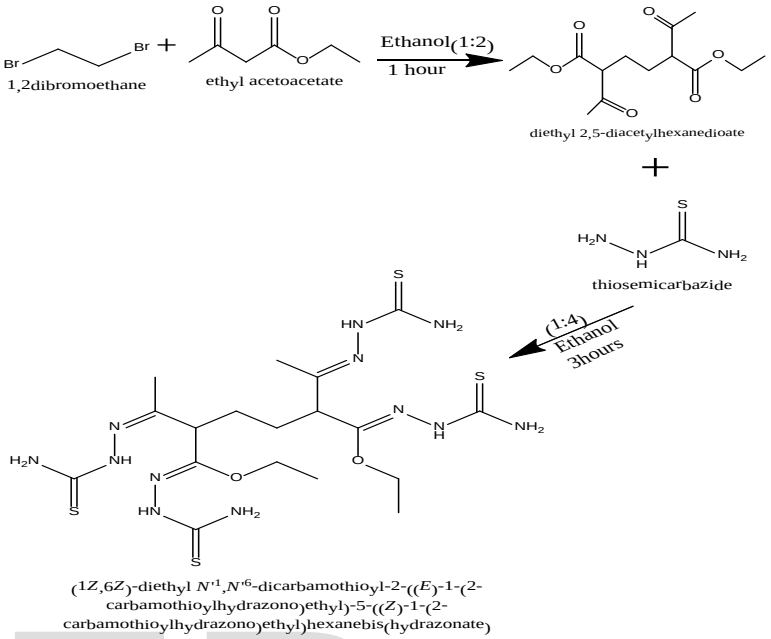

Scheme 1: Preparation of Ligand, (1Z,6Z)-diethylN'1,N'6-dicarbamothioyl-2-((E)-1-(2-carbamothioylhydrazono)ethyl)-5-((Z)1(2carbamothioylhydrazono)ethyl)hexanebis(hydrazonate)

2.2 SYNTHESIS OF METAL COMPLEXES (2)-(20)

A filtered ethanoic (50 cm^3) of $Cu(OAc)_2$. H_2O 0.96 g, 0.007 mol) was added to an ethanolic (50 cm^3) of the ligand, **(1)** (2.5 g, 0.003 mol) [1L:2M], complex **(2),** (4.68 g, 0.029 mol) $Co(OAc)_2.2H_2O$, [1L:2M], complex **(3),** (5.86 g, 0.029 mol) of $Zn(OAc)_2.2H_2O$ [1L:2M], complex **(4),** (7.72 g, 0.029 mol) of $Ni(OAc)_2.2H_2O$ [1L:2M] complex **(5),** (7.3 g, 0.029 mol) of($Ni(OAc)_2.2H_2O$, $Zn(OAc)_2.2H_2O$), [1L:1M:1M], [1L:2M], complex **(6)**, (5.96 g, 0.029 mol) of $AgNO_3$, [1L:2M], complex **(7),** (7.32 g, 0.029 mol) $Pb(NO_3)_2.2H_2O$, [1L:2M], complex **(8)**, (3.81 g, 0.029 mol) of $CuI_2.2H_2O$, [1L:2M], complex **(9),** (4.54 g, 0.029 mol) of $CuCl_2.2H_2O$, [1L:2M], complex **(10),** (4.96 g, 0,029 mol) of $SrCl_2.2H_2O$, [1L:2M], complex **(11),** (7.2 g, 0.029 mol) of $MgCl_2.3H_2O$, [1L:2M], complex **(12),** (11.52 g, 0.029 mol) of $CoCl_2.2H_2O$, [1L:2M], complex **(13),** (8.16 g, 0.029 mol) of $CuSO_4.3H_2O$, [1L:2M], complex **(14),** (5.26 g, 0.029 mol) of $NiSO_4.3H_2O$, [1L:2M], complex **(15),** (6.44 g, 0.029 mol) of $FeSO_4.3H_2O$, [1L:2M], complex **(16)**, (5.92 g, 0.029 mol) of $Al_2(SO_4)_3.2H_2O$, [1L:2M], complex **(17)**, (7.42 g, 0.029 mol) of $BaSO_4.2H_2O$, [1L:2M], complex **(18)**, (7.82 g, 0.029 mol) of $CdSO_4.2H_2O$, [1L:2M], complex **(19),** (7.84 g, 0.029 mol) of

($CuSO_4.3H_2O$, $CdSO_4.2H_2O$), [1L:2M], complx **(20)**. The mixture was refluxed with stirring for 1-3hrs range, depending on the nature of metal salts, the coloured complex was filtered off, washed with ethanol and dried under vacuo over P_4O_{10}.

. Analytical data for the ligand and prepared complexes are given in **Table (1)**:

Table 1:-Analytical and Physical Data of the Ligand [H_4L] and its Metal Complexes.

No.	Ligand/Complexes	Color	FW	M.P (°C)	Yield (%)	Anal./Found (Calc.) (%)					Molar conductance Ω
						C	H	N	M	Cl	
(1)	[H4L] $C_{18}H_{24}N_{12}O_2S_4$	White	578.18	>300	75	37.35 (37.35)	5.61 (5.92)	29.32 (29.04)	-	-	-
(2)	[(H2L)(Cu)2(OAc)4].2H2O $C_{26}H_{32}N_{12}O_{12}S_2Cu_2$	Dark gray	976.11	>300	66	31.3 (31.95)	4.88 (5.15)	17.96 (17.18)	12.95 (12.99)	-	4.92
(3)	[(H2L)(Co)2(OAc)4].2H2O $C_{26}H_{32}N_{12}O_{12}S_2Co_2$	Dark brown	968.87	>300	70	32.45 (32.23)	5.61 (5.20)	17.32 (17.35)	12.15 (12.17)	-	4.7
(4)	[(H2L)(Zn)2(OAc)4].2H2O $C_{26}H_{32}N_{12}O_{12}S_2Zn_2$	White	981.77	>300	75	31.81 (31.81)	5.50 (5.13)	17.39 (17.12)	13.33 (13.32)	-	5.73
(5)	[(H2L)(Ni)2(OAc)4].2H2O $C_{26}H_{32}N_{12}O_{12}S_2Ni_2$	Dark green	968.40	>300	79	32.89 (32.25)	5.90 (5.20)	17.72 (17.36)	12.11 (12.12)	-	3.7
(6)	[(H2L)(Ni)(Zn)(OAc)4].2H2O $C_{26}H_{32}N_{12}O_{12}S_2NiZn$	White green	975.08	>300	78	33.31 (33.03)	5.20 (5.17)	17.31 (17.24)	12.71 (12.73)	-	5.3
(7)	[(H2L)(Ag)2(NO3)4] $C_{18}H_{24}N_{12}O_{20}S_4Ag_4$	White	1258.29	>300	85	16.42 (17.18)	2.47 (2.72)	17.10 (17.81)	34.28 (34.29)	-	5.7
(8)	[(H2L)(Pb)(NO3)4].2H2O $C_{18}H_{28}N_{12}O_{18}S_4Pb_2$	White green	1278.11	>300	71	16.57 (16.93)	3.27 (3.00)	16.85 (17.55)	32.44 (32.44)	-	6.82
(9)	[(L)(Cu)2(H2O)4].2H2O $C_{18}H_{32}N_{12}O_{10}S_4Cu_2$	Black	809.95	>300	73	26.24 (26.69)	5.58 (5.25)	21.24 (20.75)	15.62 (15.69)	-	4.62
(10)	[(H2L)(Cu)2(Cl)4].2H2O $C_{18}H_{28}N_{12}S_4Cl_4O_2Cu_2$	White gray	883.74	>300	60	24.43 (24.46)	4.0 (4.33)	18.67 (19.02)	14.31 (14.38)	15.9 (16.05)	6.32

Continue table 1

No.	Ligand/Complexes	Color	FW	M.P (°C)	Yield (%)	Anal./Found (Calc.) (%)					Molar conductance Ω
						C	H	N	M	Cl	
(11)	[(H2L)(Sr)2(Cl)4].2H2O $C_{18}H_{28}N_{12}O_6S_4Cl_4Sr_2$	White yellow	931.88	>300	78	23.40 (23.20)	4.26 (4.11)	18.15 (18.04)	18.77 (18.80)	15.20 (15.22)	8.2
(12)	[(H2L)(Mg)2(Cl)4].3H2O $C_{18}H_{36}N_{12}O_7S_4Cl_4Mg_2$	Dark yellow	820.06	>300	78	25.8 (26.26)	4.72 (4.90)	19.78 (20.42)	5.88 (5.90)	17.24 (17.23)	7.56
(13)	[(H2L)(Co)2(Cl)4].2H2O $C_{18}H_{32}N_{12}O_6S_4Cl_4Co_2$	Dark brown	874.51	>300	70	23.99 (24.72)	4.51 (4.38)	19.37 (19.22)	13.46 (13.48)	16.20 (16.22)	6.38
(14)	[(H2L)(Cu)2(SO4)2(H2O)2].3H2O $C_{18}H_{40}N_{12}O_{17}S_6Cu_2$	Gray	988.10	>300	70	22.21 (21.88)	4.62 (4.49)	17.18 (17.01)	12.80 (12.86)	-	8.2
(15)	[(H2L)(Ni)2(SO4)2(H2O)2].3H2O $C_{18}H_{40}N_{12}O_{17}S_6Ni_2$	Light brown	978.39	>300	75	22.66 (22.10)	4.78 (4.53)	17.22 (17.18)	12.00 (12.00)	-	9.0
(16)	[(H2L)(Fe)2(SO4)2(H2O)2].3H2O $C_{18}H_{40}N_{12}O_{17}S_6Fe_2$	Black	970.68	>300	77	22.61 (22.27)	3.94 (4.36)	17.89 (17.32)	11.50 (11.51)	-	8.7
(17)	[(H2L)(Al)2(SO4)2(H2O)2].2H2O $C_{18}H_{40}N_{12}O_{17}S_6Al_2$	Off white	894.94	>300	70	23.89 (24.16)	4.67 (4.51)	18.61 (18.78)	6.03 (6.03)	-	7.63
(18)	[(H2L)(Ba)2(SO4)2(H2O)2].2H2O $C_{18}H_{36}N_{12}O_{16}S_6Ba_2$	White gray	1117.64	>300	70	19.28 (19.34)	3.56 (3.79)	15.16 (15.04)	24.50 (24.57)	-	7.8
(19)	[(H2L)(Cd)2(SO4)2(H2O)2].2H2O $C_{18}H_{40}N_{12}O_{18}S_6Cd_2$	White yellow	1067.81	>300	70	20.47 (20.25)	4.17 (3.96)	15.62 (15.74)	21.03 (21.05)	-	8.2
(20)	[(H2L)(Cu)(Cd)(SO4)4(H2O)2].2H2O $C_{18}H_{40}N_{12}O_{24}S_8CdCu$	Brown	1018.95	>300	68	21.30 (21.22)	4.04 (4.15)	16.36 (16.50)	17.19 (17.21)	-	8.0

Ω Ohm^{-1} cm^2 mol^{-1}

2.3 BIOLOGICAL ACTIVITY

Cytotoxic activity: Evaluation of the cytotoxic activity of the ligand and its metal complexes was carried out in the Pathology Laboratory, Pathology Department, Faculty of Medicine, El-Menoufia University, Egypt. The evaluation process was carried out invitro using the Sulfo-Rhodamine-B-stain (SRB) assay published method[14,15]. Cells were plated in 96-multiwell plate (10^4cells/well) for 24 hrs. Before treatment with the complexes to allow attachment of cell to the wall of the plate. Different concentrations of the compounds under test in DMSO (0, 5, 12.5, 25 and 50 µg/ml) were added to the cell monolayer, triplicate wells being prepared for each individual dose. Monolayer cells were incubated with the complexes for 48 hrs.at 37°C and under 5% CO_2. After 48 hrs.cells were fixed, washed and stained with Sulfo-Rhodamine-B-stain. Excess stain was wash with acetic acid and attached stain was recovered with Tris EDTA buffer. Color intensity was measured in an ELISA reader. The relation between surviving fraction and drug concentration is plotted to get the survival curve for each tumor cell line after addition the specified compound

3 RESULTS AND DISCUSSION

All the complexes are stable at room temperature, non-hydroscopic, insoluble in water and partially soluble in common organic solvents such as CHCl3, but soluble in DMF and DMSO. The analytical and physical data of the ligand and its complexes are given in Table (1), spectral data (Tables 2-6) are compatible with the proposed structures, Figure (1). The molar conductances are in the 6.3-16.4 ohm^{-1}cm^{2}mol^{-1} range, Table (1), indicating a non-electrolytic nature[24]. The high value for some complexes suggest partial dissociation in DMF. Complexes of **(1)** with metal salts using (1L: 2M) and (1L: 1M: 1M) molar ratios in ethanol gives complexes **(2)-(20)**. The composition of the complexes formed depends on metal salts and the molar ratios.

3.1 PROTON NUCLEAR MAGNETIC RESONANCE SPECTRA (1H-NMR) OF THE LIGAND (1) AND ITS ZN(II) COMPLEX (4)) ,(ZN(II) & , NI(II)) COMPLEX (6),) , SR(II) COMPLEX (11),) AND MG(II) COMPLEX (12):

The ^{1}H-NMR spectra of ligand and Complexes in deuterated DMSO show peaks consistent with the proposed structure (Scheme 1& Figure 1). The ^{1}H-NMR spectrum of the ligand and Complexes shows chemical shift observed as singlet at range (3.8-2.1) corresponding to proton of (CH_3) group[29,30], however sharp peak at 3.4 may be due to proton of solvent (CH_3OH), the peak of proton of ethoxy group (OC_2H_5) observed in ligand at 5.9ppm, which obtained in complexes at range (5.7-4.6)ppm, also chemical shift observed as singlet at 8.2 ppm (s, NH_2) which is assigned to proton of amino group adjacent to (C=S) group. The chemical shifts which appeared at range (5.3-4.2) ppm in Complexes. However, The NH

proton of hydrazide moiety (NH-N=C) of the ligand was observed at 6.1 ppm. Which appeared in complexes at range (5.7-5.1) ppm, However, The proton of methylene group $(CH_2)_2$ was observed at 6.2 ppm. Which obtained in complexes at range (6.1-5.2) ppm. The adjacent proton of (CH) was observed at 7.4 ppm. Which obtained in complexes at range (7.3-6.5) ppm[29]. By comparison the ^{1}H NMR of the ligand and the spectra of complexes, there is a significant downfield shift of the proton signal relative to the free ligand clarified that the metal ions are coordinated to the atoms or groups. This shift may be due to the formation of a coordination bond (N→) [30, 32]

3.2 MASS SPECTRA

The mass spectra of the ligand and its Zn (II) complexes **(4),** Ag(I) complexes **(7) ,** Mg(II) complexes **(12),** Al(III) complexes **(17)** and Cd(II) complex **(19)** confirmed their proposed formulations. The spectrum of ligand reveals the molecular ion peaks (m/z) at 578 amu consistent with the molecular weight of the ligand (578). Furthermore, the fragments observed at m/z = 115,134,166,220,255, 279,341,410 and 488 amu correspond to $C_5H_{11}N_2O$, $C_5H_{14}N_2O_2$, $C_5H_{14}N_2O_2S$, $C_7H_{16}N_4O_2S$, $C_9H_{19}N_4O_2S_2$, $C_9H_{21}N_6O_2S_3$, $C_{12}H_{26}N_8O_2S_3$, and $C_{14}H_{34}N_9O_2S_4$ moieties, respectively. However, the Zn (II) complex **(4)** shows peak (m/z) at 980.2 amu. Additionally, the peaks observed at 64,112,278,337,371,507,569,696,780,884, and 980 amu are due to C_3N_2, $C_4H_4N_2O_2$, $C_9H_4N_5O_4S$, $C_{11}H_{11}N_7O_4S$, $C_{13}H_{21}N_7O_4S$, and $C_{16}H_{28}N_9O_4SZn$, $C_{17}H_{30}N_9O_5S_2Zn$, $C_{19}H_{41}N_{11}O_7S_3Zn$, $C_{22}H_{43}N_{12}O_9S_3Zn$, and $C_{22}H_{50}N_{12}O_9S_4Zn_2$ moieties, respectively. Also, the Ag (I) complex **(7)** shows peak (m/z) at 1258 amu. Additionally, the peaks observed at 65,143,221,337,355, 371,410, 548,613,711,831,918, and 1208 amu are due to CH_7NS, $C_4H_3N_2S_2$, $C_6H_{13}N_4S_2O$, $C_9H_{15}N_5S_3O_3$, $C_9H_{17}N_5S_3O_4$, $C_9H_{19}N_6S_3O_4$, $C_{11}H_{20}N_7S_3O_4$, $C_{12}H_{24}N_8S_3O_4Ag$, $C_{12}H_{27}N_9S_3O_7Ag$, $C_{12}H_{33}N_{11}S_3O_{11}Ag$, $C_{13}H_{33}N_{11}S_3O_{11}Ag_2$, $C_{15}H_{36}N_{13}S_3O_{13}Ag_2$, and $C_{15}H_{36}N_{16}S_4O_{13}Ag_4$ moieties, respectively. However the Mg (II) complex **(12)** shows peak (m/z) at 823 amu. Additionally, the peaks observed at 60,91,123,266,336,367,491,583,629,696 and 762 amu are due to $C_2H_{12}N_2$, $C_2H_{12}N_2O$, $C_3H_9N_3O_2$, $C_5H_1N_4O_2$, $C_6H_{10}N_4O_3$, $C_9H_6N_4O_3$, $C_{11}H_{18}N_4O_3$, $C_{12}H_{20}N_4O_4$, $C_{17}H_{23}N_4O_4$, $C_{19}H_{24}N_4O_4$, and $C_{20}H_{30}N_4O_4$, moieties, respectively . However, the Al (III) complex **(17)** shows peak (m/z) at 894 amu. Additionally, the peaks observed at 59,117,202,313,355,411,523,655,745,833 and 894 amu are due to CHNS, $C_3H_3NS_2$, $C_6H_6N_2O_2S_2$, $C_8H_{15}N_3O_4S_3$, $C_{10}H_{17}N_3O_5S_3$, $C_{12}H_{19}N_4O_6S_3$, $C_{14}H_{29}N_5O_8S_4$, $C_{14}H_{33}N_9O_9S_5Al$, $C_{15}H_{33}N_{10}O_{11}S_6Al$, $C_{16}H_{39}N_{11}O_{13}S_6Al_2$, and $C_{18}H_{40}N_{12}O_{14}S_6Al_2$ moieties, respectively. Finaly, the Cd (II) complex **(19)** shows peak (m/z) at 1067 amu. The fragments observed at 79,93,162,212,298, 395,466,580,788,840, and 967 amu are due to CH_3O_2S, CH_3NO_2S, $C_4H_6N_2O_3S$, $C_4H_6N_2O_3S$, $C_8H_{16}N_3O_5S_2$, $C_{12}H_{21}N_5O_6S_2$, $C_{12}H_{28}N_5O_8S_3$,$C_{12}H_{30}N_5O_8S_3Cd$, $C_{15}H_{30}N_7O_{10}S_3Cd_2$, $C_{15}H_{34}N_7O_{11}S_4Cd_2$, $C_{15}H_{39}N_{10}O_{14}S_5Cd_2$, and $C_{18}H_{42}N_{12}O_{14}S_5Cd_2$, moieties.

3.3 INFRARED SPECTRA (IR)

The mode of bonding between the ligand and the metal ion revealed by comparing the IR spectra of the ligand (**1**) and its metal complexes (**2**)-(**20**). The ligand shows bands in the 3580-3507 and 3190-3100 cm^{-1} ranges, commensurate the presence of two types of intra- and intermolecular hydrogen bonds.[26]. Thus, the higher frequency band is associated with a weaker hydrogen bond and the lower frequency corresponds to stronger hydrogen bond. The medium band at at3174 cm^{-1} is assigned to v(NH) group[26,27]. The v(NH) group in the complexes appears nearly at the same region of the free ligand indicating that, the NH group is not involved in the coordination to the metal ion[28]. The peak appear at the range 3191-3167 cm^{-1}. Strong band appears at 3269 cm^{-1} is attributed to the $v(NH_2)$ group, it appear in complexes at the region 3294-3255 cm^{-1}.strong band appears at 1635 cm^{-1} is due to (C=N) group, it appears in complexes at the region 1635-1600cm^{-1}, Strong band appear at1635 cm^{-1} is due to v(C=S) band, it appear in all complex at 853-770cm^{-1} except (9) and (16) the band (C-S) appears at 770 and 820 cm^{-1} respectively. Acetate ion band appear at the range1410-1273 cm^{-1} for Complexes (**2**)-(**6**), Nitrate ion band appear at two regions, the first at the range1421-1155 cm^{-1} and the other band appear at the range875-720 cm^{-1} for Complexes (**10**)-(**13**) show bands in the region 465-403 cm^{-1} is assigned to v(M-Cl)[31]. Complexes (**2**)-(**19**) show bands in the 688-575 cm^{-1} range is assigned to v(M-O). Complexes (**2**)-(**19**) show bands in the 688-575 cm^{-1} range is assigned to v(M-O)[35].

Table 2. IR frequencies of the bands (cm^{-1}) of ligand [H_4L] and its Metal Complexes and their assignments

No.	v(H_2O)	v(NH)	V(NH_2)	v(C=N)	v(C=S)/C S	v(H bond.)	v(OAc)/SO_4/NO_3	v(M O)	v(M N)	v(M Cl)
(1)	-	3174	3272	1657	873	3576 3250, 3240-2700	-	-	-	-
(2)	3510-3100	3170	3294	1608	797	3600-3180, 3170-2500	1391,1264	623	568	-
(3)	3560-3180	3168	3276	1608	765	3610-3200, 3140-2520	1408,1300	632	599	-
(4)	3565-3182	3187	3255	1614	754	3640-3279, 3156-2515	1399,1290	622	552	-
(5)	3520-3135	3180	3255	1614	842	3540-3225, 3160-2581	1410,1276	626	512	-
(6)	3515 3110	3179	3274	1620	797	3522-3237, 3100 2535	1402,1273	665	522	-
(7)	3570-3178	3190	3257	1608	806	3525-3270, 3150-2625	1421,1155, 875,720	663	590	-
(8)	3570-3174	3171	3269	1622	790	3504-3209, 3160-2598	1408,1172, 875,790	682	576	-
(9)	3575-3160	3174	3250	1606	770	3506 3210, 3119-2512	-	683	507	-
(10)	3565 3120	3178	3272	1613	773	3512-3255, 3155-2573	-	628	584	465

Continue table 2

(11)	3523 3190	3179	3269	1635	852	3542-3254, 3184-2577	-	603	516	433
(12)	3515-3175	3184	3278	1620	800	3571-3263, 3104-2588	-	642	570	493
(13)	3507-3148	3174	3274	1631	835	3404-3213, 3114-2576	-	621	555	403
(14)	3505-3133	3179	3264	1600	808	3506-3224, 3170 2571	1194,1116, 808,690	620	539	-
(15)	3570-3119	3183	3274	1634	853	3582-3270, 3120-2560	1162,1096, 765,656	575	527	-
(16)	3580-3107	3191	2287	1640	820	3503-3290, 3190-2517	1125,1090, 702,646	616	532	-
(17)	3507-3110	3190	3282	1627	792	3520-3243, 3167-2563	1182,1101, 757,663	648	594	-
(18)	3517-3160	3170	3275	1608	843	3520-3212, 3175-2509	1175,1090, 777,660	616	505	-
(19)	3515-3172	3175	3277	1616	835	3562-3200, 3157-2586	1172,1093, 748,650	688	567	-
(20)	3560-3115	3167	3268	1622	822	3575-3274, 3137 2511	1187,1109, 783,655	605	562	-

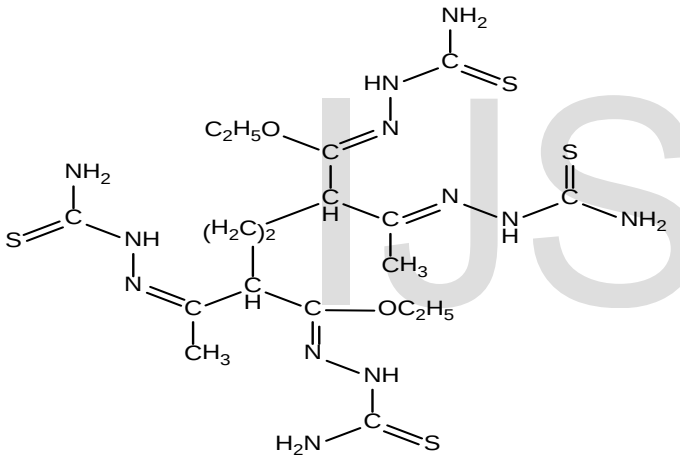

Fig.1: structure of Ligand (**1**)

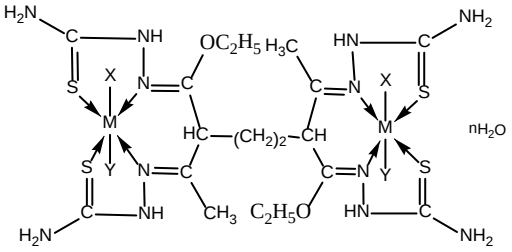

$[L(M)_2(X)_2(Y)_2].nH_2O$

M= Cu(II), X=Y= OAc, n= 2 (**2**)
M= Co(II), X=Y= OAc, n= 2 (**3**)
M= Zn(II), X=Y= OAc, n= 2 (**4**)
M= Ni(II), X=Y= OAc, n= 2 (**5**)
M= Zn(II),Ni(II) X=Y= OAc, n= 2 (**6**)
M= Pb(II), X= NO_3, n= 2 (**8**)
M= Cu(II), X=Y= H_2O, n= 2 (**9**)
M= Cu(II), X=Y=Cl, n= 2 (**10**)

$[L(M)_2(X)_2(Y)_2].nH_2O$

M= Sr(II), X=Y=Cl, n= 2 (**11**)
M= Mg(II), X=Y=Cl, n= 3 (**12**)
M= Co(II), X=Y=Cl, n= 2 (**13**)
M= Cu(II), X=SO_4, Y =H_2O, n= 3 (**14**)
M= Ni(II), X=SO_4, Y =H_2O, n= 3 (**15**)
M= Ba(II), X=SO_4, Y =H_2O, n= 2 (**18**)
M= Cd(II), X=SO_4, Y =H_2O, n= 2 (**19**)
M= Cu(II),Cd(II) X=SO_4, Y =H_2O, n= 2 (**20**)

Fig. 2: Structure representation of Cu(II), Co(II), Zn(II), Ni(II), Pb(II), Sr (I), Mg(II), Ba(II) and Cd(II) complexes (2, 3, 4, 5, 6, 8, 9, 10, 11, 12, 13, 14, 15, 18, 19, and 20)

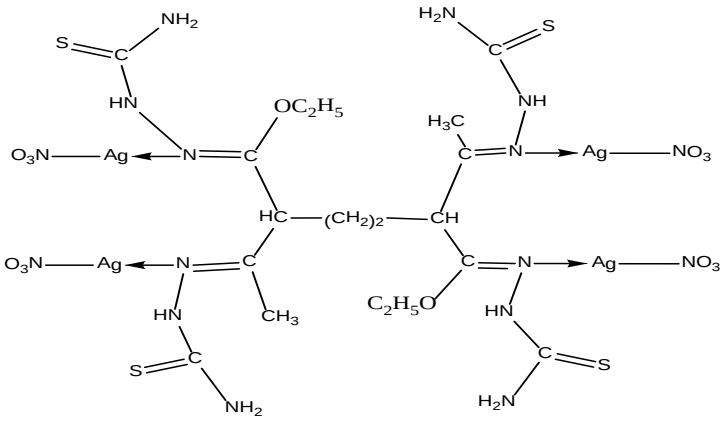

Fig. 3: Structure representation of Ag (I) complex (**7**)

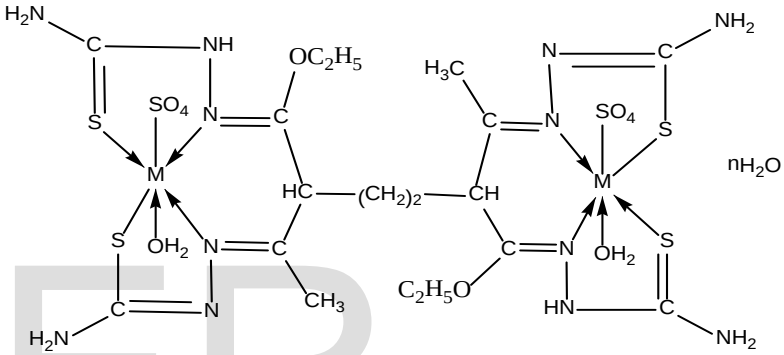

M= Fe(III), n= 3 (16) M= Al(III), n= 2 (17)

Fig. 3: Structure representation of Fe (III), and Al (III) complexes (16),and(17)

3.4 Magnetic moments

The magnetic moments of the metal complexes (**2**)-(**20**) at room temperatures are shown in (Table 4). Copper(II) complexes (**2**), (**9**), **(10) and (14**) show values in the 1.58-1.42 B.M, range corresponding to one unpaired electron in an octahedral structure[33, 34]. The low values of complexes are due to spin-spin interactions takeplace between copper(II) ions[36]. Cobalt (II) complexes (**3**) and (**13**) show values 4.28 and 4.32 B.M, indicating high spin octahedral cobalt (II) complexes[37, 38]. Iron (III) complex (**16**) shows value 6.22BM, suggesting high spin octahedral geometry around the Fe(III) ion[37, 38]. Zn(II) complexes (**4**) and (**6**), Ag(I) complex (**7**) Pb(II) complex (**8**), Ba(II) complex (**18**) Sr(II) complex (**11**) and Cd(II) complex (**19**) and (**20**) show diamagnetic property[39]. Nickel(II) complexes (**5**), **(6), and (15**) show values in the 2.27-3.21 B.M range, indicating an octahedral nickel(II) complexes[40]

3.5 Electronic spectra

The electronic spectral data for the ligand (**1**) and its metal complexes in DMF solution are summarized in Table 4. Ligand (**1**) in DMF solution shows two bands at 295 nm (log€=3.98 x 10^{-3} mol^{-1} cm^{-1}) and 315 nm (log€= 4.25x 10^{-3} mol^{-1} cm^{-1}) which may be assigned to n→π* and π→π* transitions of the immine group[36]. Copper(II)

complexes (**2**), (**9**), (**10**) and (**14**) show bands in the 235-230 and 395-305 nm ranges , these bands are due to intraligand transitions, however, the bands appear in the 495-410, 580-525 and 632-610 nm ranges, are assigned to O→Cu, charge transfer, $^2B^1 \rightarrow {}^2E$ and $^2B_1 \rightarrow {}^2B_2$ transitions, indicating a distorted tetragonal octahedral structure[41,42]. However, cobalt(II) complexes (**3**) and (**13**) show bands at 235, 323-315, 485-420, 5570 and 618 nm, the first two bands are within the ligand and the other bands are assigned to $^4T_{1g}(F) \rightarrow {}^4T_{2g}(P)(\nu_3)$, $^4T_{1g}(F) \rightarrow {}^4A_{2g}(\nu_2)$ and $^4T_{1g}(F)$ $^4T_{2g}(F)(\nu_1)$ transitions respectively indicating octahedral structure[43]. Iron(III) complex (**16**) shows bands at 238, 320, 437, 530 and 623 nm, the first two bands are within the ligand, however, the other bands are due to charge transfer and $^6A_1 \rightarrow {}^4T_1$ transitions, suggesting distorted octahedral geometry around the iron(III) ion[44,45]. Zinc(II) complexes (**4**) and (**6**), lead(II) complex (**8**), Stranchium(II) complex (**11**), Silver(I) complex (**7**), Barium(II) complex (**18**), and cadmium(II) complex **(19)** and (**20**) show bands are due to intraligand transitions. However, nickel(II) complexes (**5**), (**6**) and (**15**) show bands in the 235-237, 310-395, 478-460, 595-578, 627-625 and 780-775 nm ranges, the first three bands are within the ligand and the other bands are attributable to O→Ni charge transfer, $^3A_{2g}(F) \rightarrow {}^3T_{1g}(P)(\nu_3)$, $^3A_{2g}(F) \rightarrow {}^3T_{1g}(F)(\nu_2)$ and $^3A_{2g}(F) \rightarrow {}^3T_{2g}(F)(\nu_1)$ transitions respectively, indicating an octahedral Ni(II) geometry[41,46]. The ν_2/ν_1 ratio for (**5**), (**6**) and (**15**) are 1.24, 1.29 and 1.23, which are less than the usual range of 1.5-1.75, indicating a distorted octahedral Ni(II) complex[41,47].

Table 3: Electronic Spectra (nm) and magnetic moments (B.M) for the Ligand and Its Complexes

No.	λ_{max} (nm)	μ_{eff} in B.M.	ν_2/ν_1
(1)	295nm (log ε =3.98), 315 nm (log ε =4.25) 335(log ε= 4.59)	-	-
(2)	230,305,330,410,495,570,610	1.55	-
(3)	235,315,323,420,485,570,618	4.28	-
(4)	238,315,335,	Diamag.	-
(5)	235,310,325,395,478,585,625,780	2.37	1.24
(6)	237,320,460,595	3.21	1.29
(7)	230,310,334,365.	Diamag.	-
(8)	230,308,322	Diamag	-
(9)	235,330,345,363,445,470,525,535,625.	1. 48	-
(10)	235,315,395,475,575,618	1.58	-
(11)	235,305,325	Diamag	-
(12)	288,318,327.	Diamag	-
(13)	235,315,410,498,572,620.	4.32	-
(14)	235,318,385,465,580,632.	1.52	-
(16)	238,320,437,535,623	6.22	-
(17)	238,300,325	Diamag.	-
(18)	238,305,327	Diamag.	-
(19)	235,310,327	Diamag.	-
(20)	235,335,360,385,420,500,550,570,630.	Diamag.	-

3.6 Electron spin resonance (ESR)

The ESR spectral data for complexes (9), (13) and (20) are presented in Table 5. The spectra of copper(II) complexes (9&20) are characteristic of species d9 configuration having axial type of a d(x2-y2) ground state which is the most common for copper(II) complexes48,49. The complexes show $g_{\|} > g^{\perp} > 2.0023$, indicating octahedral geometry around copper(II) ion50,51.The g-values are related by the expression $G = (g_{\|}-2)/ (g^{\perp} -2)$50,52, where (G) exchange coupling interaction parameter (G). If G<4.0, a significant exchange coupling is present, whereas if G value > 4.0, local tetragonal axes are aligned parallel or only slightly misaligned. Complexes (**9**) and (**13**) show 2.7 and 2.4 values indicating spin-exchange interactions takeplace between copper(II) ions. This phenomena is further confirmed by the magnetic moments values (1.48 and 1.69 B.M.). The $g_{\|}/A_{\|}$ value is also considered as a diagnostic term for stereochemistry[53], the $g_{\|}/A_{\|}$ values are 168 and 238 which are expected for distorted octahedral complexes. The g-values of the copper(II) complexes with a $^2B_{1g}$ ground state ($g_{\|} > g_{\perp}$) may be expressed by[54].

$$g_{\|} = 2.002 - (8K^2_{\|}\lambda^\circ/\Delta E_{xy}) \quad (1)$$

$$g_{\perp} = 2.002 - (2K^2_{\perp}\lambda^\circ/\Delta E_{xz}) \quad (2)$$

Where $k_{\|}$ and $k_{\perp}$ are the parallel and perpendicular components respectively of the orbital reduction factor (K), λ° is the spin-orbit coupling constant for the free copper, ΔE_{xy} and ΔE_{xz} are the electron transition energies of $^2B_{1g} \rightarrow {}^2B_{2g}$ and $^2B_{1g} \rightarrow {}^2E_g$. From the above relations, the orbital reduction factors ($K_{\|}$, $K_{\perp}$, K), which are measure terms for covalency[55], can be calculated. For an ionic environment, K=1; while for a covalent environment, K<1. The lower the value of K, the greater is the covalency.

$$K^2_{\perp} = (g_{\perp} - 2.002)\, \Delta E_{xz} /2\lambda_o \quad (3)$$

$$K^2_{\|} = (g_{\|} - 2.002)\, \Delta E_{xy} /8\lambda_o \quad (4)$$

$$K^2 = (K_{2\|} + 2K^2_{\perp})/3 \quad (5)$$

K values (Table 2), for the copper(II) complexes (**9**) and(**20**) are indicating for a covalent bond character[38,56]. Kivelson and Neiman noted that, for ionic environment $g_{\|} \geq 2.3$ and for a covalent environment $g_{\|} < 2.3$[57]. Theoretical work by Smith[55] seems to confirm this view. The g-values reported here (Table 2) show considerable covalent bond character[38]. Also, the in-plane σ-covalency parameter, $\alpha^2(Cu)$ was calculated by

$$\alpha^2(Cu) = (A_{\|}/0.036) + (g_{\|} - 2.002) + 3/7(g - 2.002) + 0.04 \quad (6)$$

The calculated values (Table 2) suggest a covalent bonding[38,56]. The in-plane and out of- plane π- bonding coefficients β_1^2 and β_2^2 respectively, are dependent upon the values of ΔE_{xy} and ΔE_{xz} in the following equations[58].

$$\alpha^2\beta^2 = (g_{\perp} - 2.002)\, \Delta E_{xy}/2\lambda_o \quad (7)$$

$$\alpha^2\beta_1^2 = (g_{\|} - 2.002)\, \Delta E_{xz}/8\lambda_o \quad (8)$$

In this work, the complexes (**9**), and (**13**) show β_1^2 values 0.89, 0 and 1.08 indicating a moderate degree of covalency in the in-plane π-bonding[56,59]. β^2 value for complexes (**9**), (**13**) show 1.43 and 1.92 indicating ionic character of the out-of-plane[56,59]. It is possible to calculate approximate orbital populations ford orbitals[60] by

$A_{\parallel} = A_{iso} - 2B[1 \pm (7/4)\,\Delta g_{\parallel}]\ \Delta g_{\parallel} = g_{\parallel} - g_e$ (9)

$a^2 d = 2B/\ 2B°$ (10)

Where A° and 2B° is the calculated dipolar coupling for unit occupancy of d orbital respectively. When the data are analyzed, the components of the ^{60}Cu hyperfine coupling were considered with all the sign combinations. The only physically meaningful results are found when $A_{\parallel}$ and $A_{\perp}$ were negative. The resulting isotropic coupling constant was negative and the parallel component of the dipolar coupling 2B are negative (-136.4, 0 and -102 G). These results can only occur for an orbital involving the d_{x2-y2} atomic orbital on copper. The value for 2B is quite normal for copper(Il) complexes[61]. The $|A_{iso}|$ value was relatively small. The 2B value divided by $2B^o$ (The calculated dipolar coupling for unit occupancy of d_{x2-y2} (235.11 G), using equation (10) suggests all orbital population are 59 and 43% d-orbital spin density, clearly the orbital of the unpaired electron is d_{x2-y2}[62]. The ESR spectrum of cobalt(II) complex (**13**) at room temperature shown an isotropic value (g_{iso}= 2.09).

$G=(g_{11} -2)/(g_{\perp}-2)$

Table 4: ESR data for metal (II) complexes

Complex	$g_{\parallel}$	$g_{\perp}$	g_{iso}[a]	$A_{\parallel}$ (G)	$A_{\perp}$ (G)	A_{iso}[b] (G)	G[c]	ΔE_{xy} (cm^{-1})	ΔE_{xz} (cm^{-1})	$K_{\perp}^2$	$K_{\parallel}^2$	K^2	K	$g_{\parallel}/A_{\parallel}$ (cm^{-1})	α^2	β^2	β_1^2	-2β	a^2d (%)
(9)	2.19	2.07	2.11	130	10	50	2.7	18182	21277	0.87	0.554	076	0.87	168	0.61	1.43	0.89	136.4	59
(13)	-	-	2.09	-	-	-	-	-	-	-	-	-	-	-	-	-	-	-	-
(20)	2.22	2.09	2.13	90	15	40	2.4	18182	20000	1.059	0.597	0.9	0.94	238	0.55	1.92	1.08	102	43

[a]g_{iso}= (2$g_{\perp}$+$g_{\parallel}$)/3,[b]A_{iso}=(2$A_{\perp}$+$A_{\parallel}$)/3,[C]G=($g_{\parallel}$-2)/($g_{\perp}$-2) (12), (13)

3.7 Thermal analyses (Differential Thermal Analysis (DTA) and Thermo Gravimetric Analysis (TGA))

Since the IR spectra indicate the presence of water molecules, thermal analyses (DTA and TGA) were carried out to certain their nature. The thermal curves in the temperature 27-600°range for complexes (**5**), (**6**), (**11**), (**14**) and (**18**) are thermally stable up to 45 °C. Broken of hydrogen bondings occurs as endothermic peak within the temperature 45-50 °C as shown in Table 6. Dehydration is characterized by endothermic peaks within the temperature 80-85°C range, corresponding to the loss of hydrated water molecules as in complexes (**5**) and (**14**). The elimination of coordinated water molecules occur in 145-180°C range accompanied by endothermic peaks as in complexes (**14**), and (**18**)[67,68]. The thermogram of Ni(II) complex (**5**) showed that, the complexes decomposed in five step. The first occurred at 45°C with no weight loss as endothermic peak, may be due to break of hydrogen bondings. The second step occur at 85°C with 3.44 % weight loss (Calc. 3.72%) as endothermic peak which could be due to the elimination of two hydrated water molecules. The decomposition step which occurred at 280°C with 25.1% weight loss (Calc. 25.4%) could be due to the elimination of four coordinated acetate groups. The complex shows an endothermic peak observed at 360°C is due its melting point. Finally, exothermic peaks appear at 360,455,480, and 515 °C corresponding to oxidative thermal decomposition which proceeds slowly with leaving NiO with 22.06% weight loss (Calc. 21.3%)[69]. The thermogram of Ni(II) and Zn(II) Complex (**6**) shows endothermic peak at 80 with 3.6% weight loss (Calc. 3.5%) are assigned to two hydrated water molecules. The endothermic peak observed at 280 with 25.4% weight loss (Calc. 25.1%), could be due to the elimination of four acetate ions. Another exothermic peak observed at 320 with no weight loss may be due to its melting point. Finally, the complex shows endothermic peaks at 520,575 and 640°C with 21.8% weight loss (Calc. 21.9%) corresponding to oxidative thermal decomposition which proceeds slowly with final residue, assigned to NiO and ZnO[70]. The thermogram of Sr(II) complex (**11**) shows endothermic peak at 45°C, due to break of hydrogen bonding. The second step occur at 155°C with 15.8 % weight loss (Calc. 15.8%) as endothermic peak which could be due to loss of two hydrated water molecules. Another endothermic peak appeared at 80°C, with 3.7% weight loss (Calc. 3.8%), due to the elimination of two coordinated chloride ions. The complex displayed another endothermic peak at 302°C may be assigned to its melting point. Oxidative thermal decomposition occurs in the 450,566, and 648°C with exothermic peaks, leaving SrO with 13.7% weight loss (Calc. 13.8%)[69]. The thermogram ofCu(II) complex (**14**) shows endothermic peak at 45°C, is due to break of hydrogen bondings, Another endothermic peak at 85°C with 5.3% weight loss (Calc. 5.4%) is assigned to the loss of three hydrated water molecules. The third step occur at 180°C with 3.9% weight loss (Calc. 3.8%) as endothermic peak which could be due to the elimination of two coordinated water molecules. Another endothermic peak at 315 with 21.2% weight loss (Calc. 21.3%) is due to loss of two coordinated sulphate ions. At 380°C, endothermic peak appeared which is due to melting point. Oxidative thermal decomposition occurs at 469,480 and 500 °C with exothermic peaks, leaving CuO with 11.3% weight loss (Calc. 11.2%)[69]. The thermogramof Ba(II) complex (**18**) shows an endothermic peak at 55°C due to break of hydrogen bondings and another endothermic beak at 80 °C, with 3.08% weight loss (Calc. 3.22%) due to loss of two hydrated water molecule. The endothermic peak observed at 145°C with 3.08% weight loss (Calc. 3.22%), is assigned to loss of two coordinated water molecules. The endothermic peak observed at 335°C with 18.5% weight loss (Calc. 18.3%) is due to loss of two coordinated sulphate group. Another exothermic peak observed at 420°C may be assigned to its melting point. Oxidative thermal decomposition occurs at 485,535, and 585°C with exothermic peaks, leaving BaO with 19.7% weight loss (Calc. 19.8%)[69]. The thermal data are present in table 5**.**

Table 5: Thermal analyses for metal (II) complexes

Compound No. Molecular formula	Temp. (C)	DTA (peak)		TGA (Wt.loss %)		Assignments
		Endo	Exo	Calc.	Found	
Complex (5) $[(H_4L)(Ni)_2(OAc)_4].2H_2O$ $C_{26}H_{50}N_{12}O_{12}S_4Ni_2$	45	Endo	-	-	-	Broken of H-bondings
	85	Endo	-	3.72	3.44	Loss of ($2H_2O$) hydrated water molecules
	285	Endo	-	25.3	24.8	Loss of four coordinated acetate group
	360	-	Exo	-	-	Melting point
	360,455, 480,515	-	Exo	21.3	22.06	Decomposition process with the formation of 2NiO
Complex (6) $[(H_4L)(Ni)(Zn)(OAc)_4].2H_2O$ $C_{26}H_{50}N_{12}O_{12}S_4NiZn$	50	Endo	-	-	-	Broken of H-bondings
	80	Endo	-	3.7	3.6	Loss of ($2H_2O$) hydrated water molecules
	280	Endo	-	25.1	25.4	Loss of four coordinated acetate group
	320	Endo	-	-	-	Melting point
	520,575, 640	-	Exo	21.9	21.8	Decomposition process with the formation of ZnO&NiO
Complex (11) $[(H_4L)(Sr)_2(Cl)_4].2H_2O$ $C_{18}H_{38}N_{12}O_4S_4Cl_4Sr_2$	45	Endo	-	-	-	Broken of H-bondings
	80	Endo	-	3.8	3.7	Loss of ($2H_2O$) hydrated water molecules
	155	Endo	-	15.8	15.8	Loss of 2 coordinated Cl Ion
	302	Endo	-	-	-	Melting point
	450,566, 648	-	Exo	13.8	13.7	Decomposition process with the formation of 2SrO
Complex (14) $[(H_4L)(Cu)_2(SO_4)_2(H_2O)_2].3H_2O$ $C_{14}H_{44}N_{12}O_{15}S_6C_{u2}$	48	Endo	-	-	-	Broken of H-bondings
	85	Endo	-	5.4	5.3	Loss of ($3H_2O$) hydrated water molecules
	180	Endo	-	3.8	3.9	Loss of ($2H_2O$) coordinated water molecules
	315	Endo	-	21.3	21.2	Loss of two coordinated sulphate group
	380	Endo	-	-	-	Melting point
	469,480, 500	-	Exo	11.2	11.3	Decomposition process with the formation of 2CuO
Complex (18) $[(H_4L)(Ba)_2(SO_4)_2(H_2O)_2].2H_2O$ $C_{14}H_{40}N_{12}O_{14}S_6Ba_2$	55	Endo	-	-	-	Broken of H-bondings
	80	Endo		3.22	3.08	Loss of ($2H_2O$) hydrated water molecules
	145	Endo	-	3.33	3.08	Loss of ($2H_2O$) coordinated water molecules
	335	Endo	-	18.3	18.5	Loss of two coordinated sulphate group
	420	Endo	-	-	-	Melting point
	485,535, 585	-	Exo	19.8	19.7	Decomposition process with the formation of 2BaO

3.8 CHEMOTHERAPEUTIC STUDIES

The biological activity of the ligand (1) and its metal complexes (4), (7), (9), and (19) were evaluated against HEPG-2 cell line. In this study, we try to know the chemotherapeutic activity of the tested complexes by comparing them with the standard drug (Vinblastine sulphate). The treatment of the different complexes in DMSO showed similar effect in the tumoral cell line used as it was previously reported71. The solvent dimethyl sulphoxide (DMSO) shows no effect in cell growth. The ligand (1) shows a weak inhibition effect at ranges of concentrations used, however, the complexes showed better effect against HEPG-2 cell lines. The obtained data indicate the surviving fraction ratio against HEPG-2 tumor increasing with the decrease of the concentration in the range of the tested concentrations69. Cytotoxicity results indicated that the tested complexes (4), (7), (9), and (19) demonstrated potent. Copper(II) complex (9) showed the highest cytotoxicity effect against cell line with IC50 value of 3.82 µM, and then complex (19) with IC50 value 2.43 µM..This can be explained as Cu(II) ion binds to DNA. It seems that, changing the anion and the nature of the metal ion has effect on the biological behavior, due to alter Binding ability of DNA binding, so testing of different complexes is very interesting from this point of view. Chemotherapeutic activity of the complexes may be attributed to the central metal atom which was explained by Tweedy's chelation theory71,72. Also, the positive charge of the metal increases the acidity of coordinated ligand that bears protons, leading to stronger hydrogen bonds which enhance the biological activity73,74. The cytotoxic effect of the ligand and its HEPG-2 metal complexes are presented in table 6.

Table 6: Order of cytotoxic effect of the studied complexes against HEPG-2 cell line

concentration	**Order of cytotoxic effect of studied complex (HEPG-2 cell line)**
500 µg/ml	**(9)> Std>(19)>(4)>(7)**
250 µg/ml	**(9)> Std>(19)>(4)>(7)**
62.5 µg/ml	**(9)> Std>(19)>(7)>(4)**
15.6 µg/ml	**(9)> (4)>(19)>(7)> Std**
3.9 µg/ml	**(9)> (4)>(19)>(7)> Std**
1.0 µg/ml	**(9)> (4)>(19)>(7)> Std**

Fig. 4: Evaluation of cytotoxicity of metal complexes against human hepatic HEPG-2 Cell Line

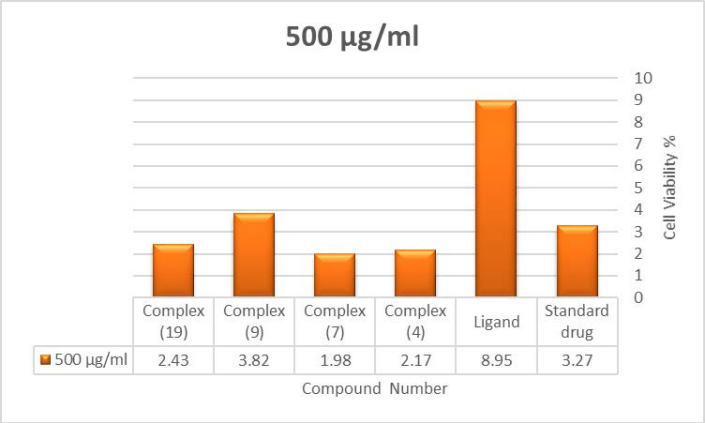

Fig. 5: Evaluation of cytotoxicity of metal complexes against human hepatic HEPG-2 Cell Line at 500 µg/ml

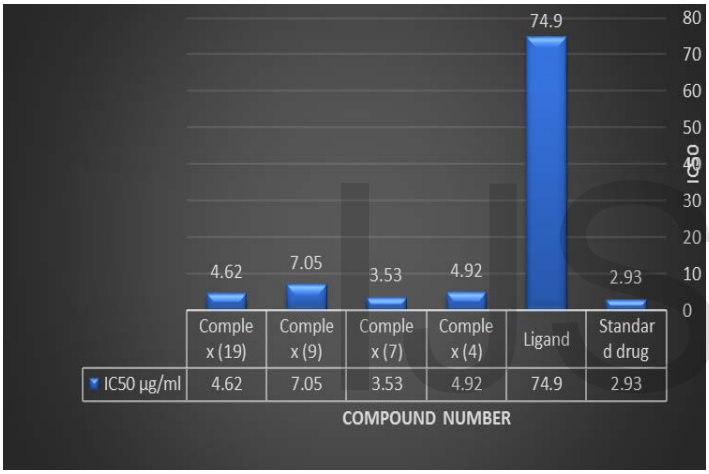

Fig. 6: IC_{50} values of ligand and it, s complexes **(4), (7), (9), and (19)** against human hepatic HEPG-2 cell lines.

REFERENCES

[1] Sutradhar, M., Barman, T. R., & Rentschler, E. (2014). Coordination versatility of 1, 5-bis (salicylidene) carbohydrazide in Ni (II) complexes. *Inorganic Chemistry Communications*, 39, 140-143.

[2] Sharif, Z. I. M., Mustapha, F. A., Jai, J., Yusof, N. M., & Zaki, N. A. M. (2017). Review on methods for preservation and natural preservatives for extending the food longevity. *Chemical Engineering Research Bulletin*, *19*, 145-153.

[3] Hossain, M. S., Roy, P. K., Zakaria, C. M., & Kudrat-E-Zahan, M. (2018). Selected Schiff base coordination complexes and their microbial application*: A review. IJCS*, 6(1), 19-31.

[4] Singh, M., Singh, S. K., Gangwar, M., Nath, G., & Singh, S. K. (2016). Design, synthesis and mode of action of novel 2-(4-aminophenyl) benzothiazole derivatives bearing semicarbazone and thiosemicarbazone moiety as potent antimicrobial agents. Medicinal Chemistry Research, 25(2), 263-282.GERDEMANN, C., EICKEN, C. & KREBS, B. 2002. The crystal structure of catechol oxidase: new insight into the function of type-3 copper proteins. *Accounts of chemical research*, 35, 183-191.

[5] .M.C Rodriguez-Arguelles, E.C Lopez-Silva, J.Sanmartin, et al. Copper complexes of imidazole-2-, pyrrole-2- and indol-3-carbaldehyde thiosemicarbazones: inhibitory activity against fungi and bacteria. J Inorg Biochem. 2005; 99:2231–9.GIELEN, M. & TIEKINK, E. R. 2005. Metallotherapeutic drugs and metal-based diagnostic agents: the use of metals in medicine, John Wiley & Sons.

[6] N.C Saha, C.Biswas , A. Ghorai , et al. Synthesis, structural characterisation and cytotoxicity of new iron(III) complexes with pyrazolyl thiosemicabazones. Polyhedron. 2012;34:1–12.

[7] M Riyadh, S., M Gomha, S., & A Mahmmoud, E. (2017). Utility of Ethylidenethiosemicarbazides in Heterocyclic Synthesis. *Current Organic Synthesis*, *14*(1), 3-21.

[8] M.F Brana, A.Gradillas ,A.G Ovalles , et al. Synthesis and biological activity of N, N-dialkylaminoalkyl-substituted bisindolyl and diphenyl pyrazolone derivatives. *Bioorg Med Chem. 2006;* 14:9–16.

[9] . Pahontu, E., Julea, F., Rosu, T., Purcarea, V., Chumakov, Y., Petrenco, P., & Gulea, A. (2015). Antibacterial, antifungal and in vitro antileukaemia activity of metal complexes with thiosemicarbazones. *Journal of cellular and molecular medicine*, 19(4), 865-878.

[10] Palanimurugan, A., & Kulandaisamy, A. (2018). DNA, in vitro antimicrobial/anticancer activities and biocidal based statistical analysis of Schiff base metal complexes derived from salicylalidene-4-imino-2, 3-dimethyl-1-phenyl-

3-pyrazolin-5-one and 2-aminothiazole. Journal of Organometallic Chemistry.

[11] Kavitha, P., Chary, M. R., Singavarapu, B. V. V. A., & Reddy, K. L. (2016). Synthesis, characterization, biological activity and DNA cleavage studies of tridentate Schiff bases and their Co (II) complexes. Journal of Saudi Chemical Society, 20(1), 69-80.COLLEE, J. 1989. *Mackie and McCartney practical medical microbiology*.

[12] Subarkhan, M. M., Prabhu, R. N., Kumar, R. R., & Ramesh, R. (2016). Antiproliferative activity of cationic and neutral thiosemicarbazone copper (II) complexes. *RSC Advances*, *6*(30), 25082-25093.

[13] Pahontu, E., Julea, F., Rosu, T., Purcarea, V., Chumakov, Y., Petrenco, P., & Gulea, A. (2015). Antibacterial, antifungal and in vitro antileukaemia activity of metal complexes with thiosemicarbazones. *Journal of cellular and molecular medicine*, *19*(4), 865-878.

[14] Pahontu, E., Julea, F., Rosu, T., Purcarea, V., Chumakov, Y., Petrenco, P., & Gulea, A. (2015). Antibacterial, antifungal and in vitro antileukaemia activity of metal complexes with thiosemicarbazones. *Journal of cellular and molecular medicine*, *19*(4), 865-878.

[15] Pahontu, E., Julea, F., Rosu, T., Purcarea, V., Chumakov, Y., Petrenco, P., & Gulea, A. (2015). Antibacterial, antifungal and in vitro antileukaemia activity of metal complexes with thiosemicarbazones. *Journal of cellular and molecular medicine*, 19(4), 865-878.

[16] . Pahontu, E., Julea, F., Rosu, T., Purcarea, V., Chumakov, Y., Petrenco, P., & Gulea, A. (2015). Antibacterial, antifungal and in vitro antileukaemia activity of metal complexes with thiosemicarbazones. *Journal of cellular and molecular medicine*, 19(4), 865-878.

[17] Zhu, T., Shen, S., Lu, Q., Ye, X., Ding, W., Chen, R., ... & Wu, W. (2017). Design and synthesis of novel N (4)-substituted thiosemicarbazones bearing a pyrrole unit as potential anticancer agents. *Oncology letters*, 13(6), 4493-4500.

[18] Pandya, J. H., Jadeja, R. N., & Ganatra, K. J. (2014). Spectral characterization and biological evaluation of Schiff bases and their mixed ligand and metal complexes derived from 4, 6-diacetylresorcinol. *Journal of Saudi Chemical Society*, *18*(3), 190-199.

[19] Abuelizz, H. A., Dib, R. E., Marzouk, M., Anouar, E. H., A Maklad, Y., N Attia, H., & Al-Salahi, R. (2017). Molecular docking and anticonvulsant activity of newly synthesized quinazoline derivatives. Molecules, 22(7), 1094.

[20] Viñuelas-Zahínos, E., Luna-Giles, F., Torres-García, P., & Fernández-Calderón, M. C. (2011). Co (III), Ni (II), Zn (II) and Cd (II) complexes with 2-acetyl-2-thiazoline thiosemicarbazone: Synthesis, characterization, X-ray structures and antibacterial activity. *European journal of medicinal chemistry*, 46(1), 150-159.

[21] Halder, S., Paul, P., Peng, S. M., Lee, G. H., Mukherjee, A., Dutta, S., ... & Bhattacharya, S. (2012). Benzaldehyde thiosemicarbazone complexes of platinum: Syntheses, structures and cytotoxic properties. Polyhedron, 45(1), 177-184.

[22] Sharif, Z. I. M., Mustapha, F. A., Jai, J., Yusof, N. M., & Zaki, N. A. M. (2017). Review on methods for preservation and natural preservatives for extending the food longevity. *Chemical Engineering Research Bulletin*, 19, 145-153.

[23] West D.X., Liberta A.E., padhye S.B., Chikata R.C.,Sonawana P.B., Kumbhar A.S. and Yerande R.G., *coord.chem.Rev.*, 123,49(1993)

[24] Mulazimoglu, A. D., Mulazimoglu, I. E., & Mercimek, B. (2009). Synthesis, Characterizations and Investigation of Electrochemical Behaviours of 4-[(2-Hydroxyphenylimino) methyl] benzene-1, 3-diol. *Journal of Chemistry*, *6*(4), 965-974.

[25] El-Gammal, O. A., El-Reash, G. A., & Ahmed, S. F. (2015). Synthesis, spectral characterization, molecular modeling and in vitro antibacterial activity of complexes designed from O2, NO and NO donor Schiff-base ligand. Spectrochimica Acta Part A: Molecular and *Biomolecular Spectroscopy*, 135, 227-240.

[26] Kotarba, M. J., & Nagao, K. (2015). Molecular and

isotopic compositions and origin of natural gases from Cambrian and Carboniferous-Lower Permian reservoirs of the onshore Polish Baltic region. *International Journal of Earth Sciences*, 104(1), 241-261.

[27] El-Tabl, A. S., El-wahed, M. M. A., & Rezk, A. M. S. M. (2014). Cytotoxic behavior and spectroscopic characterization of metal complexes of ethylacetoacetate bis (thiosemicarbazone) ligand. Spectrochimica Acta Part A*: Molecular and Biomolecular Spectroscopy*, 117, 772-788.

[28] Khan, S. A., Imam, S. M., Ahmad, A., Basha, S. H., & Husain, A. (2017). Synthesis, molecular docking with COX 1& II enzyme, ADMET screening and in vivo anti-inflammatory activity of oxadiazole, thiadiazole and triazole analogs of felbinac. *Journal of Saudi Chemical Society.*

[29] El-Saied, F. A., Al-Hakimi, A. N., Wahba, M. A., & Shakdofa, M. M. E. (2017). Preparation, Characterization and Antimicrobial Activities of N'-((3-(hydroxyimino) butan-2-ylidene)-2 (phenylamino) acetohydrazide and Its Metal Complexes. *Egyptian Journal of Chemistry*, *60*(1), 1-24.

[30] Singh, D. P., Raghuvanshi, D. S., Singh, K. N., & Singh, V. P. (2013). Synthesis, characterization and catalytic application of some novel binuclear transition metal complexes of bis-(2-acetylthiophene) oxaloyldihydrazone for C N bond formation. *Journal of Molecular Catalysis A: Chemical*, 379, 21-29.

[31] El-Tabl, A. S., El-Hofy, M. I., Anwar, A. M., & Mohamed, H. A. (2013). Metal (II) complexes of oxime ligand: synthesis, characterization and biological activity. Blue Biotechnology *Journal, 2(2), 319.*

[32] Pisk, J., Daran, J. C., Poli, R., & Agustin, D. (2015). Pyridoxal based ONS and ONO vanadium (V) complexes: Structural analysis and catalytic application in organic solvent free epoxidation. *Journal of Molecular Catalysis A: Chemical*, 403, 52-63.

[33] El-Tabl, A. S., Mohamed Abd El-Waheed, M., Wahba, M. A., & El-Fadl, A. E. H. A. (2015). Synthesis, characterization, and anticancer activity of new metal complexes derived from 2-hydroxy-3-(hydroxyimino)-4-oxopentan-2-ylidene) benzohydrazide. Bioinorganic chemistry and applications, 2015.

[34] El-Tabl, A. S., Abd-El Wahed, M. M., Wahba, M. A., Shakdofa, M. M., & Gafer, A. (2016). Bimetallic Transition Metal Complexes of 2, 3-Dihydroxy-N', N'4-bis ((2-Hydroxynaphthalen-1-yl) Methylene) Succinohydrazide Ligand as a New Class of Bioactive Compounds; Synthesis, Characterization and Cytotoxic Evaluation. *Indian Journal of Advances in Chemical Science*, *4*(1), 114-29..

[35] El-Tabl, A. S., El-wahed, M. M. A., & Rezk, A. M. S. M. (2014). Cytotoxic behavior and spectroscopic characterization of metal complexes of ethylacetoacetate bis (thiosemicarbazone) ligand. Spectrochimica Acta Part A: *Molecular and Biomolecular Spectroscopy*, 117, 772-788.

[36] El-Tabl, A. S., El-wahed, M. M. A., & Rezk, A. M. S. M. (2014). Cytotoxic behavior and spectroscopic characterization of metal complexes of ethylacetoacetate bis (thiosemicarbazone) ligand. Spectrochimica Acta Part A*: Molecular and Biomolecular Spectroscopy*, 117, 772-788.

[37] . El-Tabl, A. S., El-Wahed, M. M. A., & El-Razek, S. E. A. (2013). Preparation, spectroscopic investigation and antiproliferative capacity of new metal complexes of (3E)-2-(hydroxyimino)-NP-Tolyl-3-(P-tolylimino)
butanamide. *Spectrochimica Acta Part A: Molecular and Biomolecular Spectroscopy*, *105*, 600-611.

[38] El-Tabl, A. S., El-wahed, M. M. A., & Rezk, A. M. S. M. (2014). Cytotoxic behavior and spectroscopic characterization of metal complexes of ethylacetoacetatebis (thiosemicarbazone) ligand. Spectrochimica Acta Part A*: Molecular and Biomolecular Spectroscopy*, 117, 772-788.

[39] Emam, S. M., Abdou, S., Ahmed, H. M., & Emad, E. A. (2017). Synthesis, structural characterization, electrochemical and biological studies on divalent metal chelates of a new ligand derived from pharmaceutical preservative, dehydroacetic acid, with 1, 4-

diaminobenzene. Arabian *Journal of Chemistry*, 10, S3816-S3825.

[40] Abdou, S., Abd-El Wahed, M. M., Wahba, M. A., Shakdofa, M. M., & Abu-Setta, M. H. *Journal of Chemical, Biological and Physical Sciences*.

[41] Abdel-Monem, Y. K., El-Enein, S. A. A., & El-Sheikh-Amer, M. M. (2017). Design of new metal complexes of 2-(3-amino-4, 6-dimethyl-1H-pyrazolo[3,4-b]pyridin-1-yl)aceto-hydrazide: synthesis, characterization, modelling and antioxidant activity. *Journal of Molecular Structure*, 1127, 386-396.

[42] Abdou, S., Abd-El Wahed, M. M., Wahba, M. A., Shakdofa, M. M., & Abu-Setta, M. H. *Journal of Chemical, Biological and Physical Sciences.*

[43] Singh, U., Bukhari, M. N., Anayutullah, S., Alam, H., Manzoor, N., & Hashmi, A. A. (2016). Synthesis, Characterization and Biological Evaluation of Metal Complexes with Water-Soluble Macromolecular Dendritic Ligand. *Pharmaceutical Chemistry Journal*, 49(12), 868-877.

[44] Hassoon, A. A., Al-Radadi, N. S., Nawar, N., & Mostafa, M. M. (2016). New Square-Pyramidal Oxovanadium (IV) Complexes Derived from Polydentate Ligand (L1). *Open Journal of Inorganic Chemistry*, 6(01), 23.

[45] Hosny, N. M., Hassan, N. Y., Mahmoud, H. M., & Abdel-Rhman, M. H. (2018). Spectral, optical and cytotoxicity studies on 2-isonicotinoyl-N-phenylhydrazine-1-carboxamide (H3L) and some of its metal complexes. *Journal of Molecular Structure*, *1156*, 602-61.

[46] Thakkar, N. V., & Bootwala, S. Z. (1995). Synthesis and characterization of binuclear metal complexes derived from some isonitrosoacetophenones and benzidine

[47] El-Tabl, A. S., El-wahed, M. M. A., & Rezk, A. M. S. M. (2014). Cytotoxic behavior and spectroscopic characterization of metal complexes of ethylacetoacetate bis (thiosemicarbazone) ligand. Spectrochimica Acta Part A: *Molecular and Biomolecular Spectroscopy*, 117, 772-788.

[48] El-Saied, F. A., Salem, T. A., Aly, S. A., & Shakdofa, M. M. E. (2017). Evaluation of Anti-Hyperglycemic Effect of Synthetic Schiff Base Vanadium (IV) Complexes. *Pharmaceutical Chemistry Journal*, 51(9), 833-842.

[49] El-Tabl, A. S., El-wahed, M. M. A., & Rezk, A. M. S. M. (2014). Cytotoxic behavior and spectroscopic characterization of metal complexes of ethylacetoacetate bis (thiosemicarbazone) ligand. Spectrochimica Acta Part A: *Molecular and Biomolecular Spectroscopy*, 117, 772-788.

[50] El-Tabl, A. S., El-Wahed, M. M. A., & El-Razek, S. E. A. (2013). Preparation, spectroscopic investigation and antiproliferative capacity of new metal complexes of (3E)-2-(hydroxyimino)-NP-Tolyl-3-(P-tolylimino) butanamide. Spectrochimica Acta Part A: *Molecular and Biomolecular Spectroscopy*, 105, 600-611.

[51] El-Tabl, A. S., El-wahed, M. M. A., & Rezk, A. M. S. M. (2014). Cytotoxic behavior and spectroscopic characterization of metal complexes of ethylacetoacetate bis (thiosemicarbazone) ligand. Spectrochimica Acta Part A: *Molecular and Biomolecular Spectroscopy*, 117, 772-788.

[52] Devi, S. P., Shantibala Devi, N., Singh, L. J., Devi, R. B., Devi, W. R., Singh, C. B., & Singh, R. H. (2017). Spectroscopic and DNA interaction studies on mixed ligand copper (II) complexes of dicyanamide with ethylenediamine or 1, 3-diaminopropane. *Inorganic and Nano-Metal Chemistry*, 47(2), 223-233.

[53] Yan, L., Lu, Y., & Li, X. (2016). A density functional theory protocol for the calculation of redox potentials of copper complexes. *Physical Chemistry Chemical Physics*, 18(7), 5529-5536.

[54] Soodan, R. K., Pakade, Y. B., Nagpal, A., & Katnoria, J. K. (2014). Analytical techniques for estimation of heavy metals in soil ecosystem: *A tabulated review*. Talanta, 125, 405-410.

[55] . El-Tabl, A. S., Shakdofa, M. M., & Shakdofa, A. M. (2013). Metal complexes of N'-[2-hydroxy-5-(phenyldiazenyl)-benzylidene] isonicotinohydrazide. Synthesis, spectroscopic characterization and antimicrobial activity. *Journal of the Serbian Chemical Society*, 78(1), 39.

[56] Abdel-Rahman, L. H., El-Khatib, R. M., Nassr, L. A., Abu-Dief, A. M., Ismael, M., & Seleem, A. A. (2014). Metal based pharmacologically active agents: synthesis, structural characterization, molecular modeling, CT-DNA binding studies and in vitro antimicrobial screening of iron (II) bromosalicylidene amino acid chelates. Spectrochimica Acta Part A: *Molecular and Biomolecular Spectroscopy*, 117, 366-378.

[57] Anacona, J. R., Noriega, N., & Camus, J. (2015). Synthesis, characterization and antibacterial activity of a tridentate Schiff base derived from cephalothin and sulfadiazine, and its transition metal complexes. Spectrochimica Acta Part A: *Molecular and Biomolecular Spectroscopy*, 137, 16-22.

[58] Saad El-Tabl, A., Abd-Elwahed, M., & Hemid Mohammed, M. (2013). Synthesis, spectral characterisation and cytotoxic effect of metal complexes of 2-(2-(4-carboxyphenyl) guanidino) acetic acid ligand. *Chemical Speciation & Bioavailability*, 25(2), 133-146.

[59] El-Tabl, A. S., Stephanos, J. J., Abd-Elwahed, M. M., & El-Gamasy, S. M. (2013). Novel metal complexes of guanidine ligand; Synthesis, Spectroscopic Characterization and Biological Activity. *Int. J. Chem Tech Res*, 5(1), 430-449.

[60] El-Tabl, A. S., El-wahed, M. M. A., & Rezk, A. M. S. M. (2014). Cytotoxic behavior and spectroscopic characterization of metal complexes of ethylacetoacetate bis (thiosemicarbazone) ligand. Spectrochimica Acta Part A: *Molecular and Biomolecular Spectroscopy*, 117, 772-788.

[61] Abdou, S., Abd-El Wahed, M. M., Wahba, M. A., Shakdofa, M. M., & Abu-Setta, M. H. *Journal of Chemical, Biological and Physical Sciences.*

[62] Shakdofa, M. M., Al-Hakimi, A. N., Elsaied, F. A., Alasbahi, S. O., & Alkwlini, A. M. A. (2017). Synthesis, characterization and bioactivity of Zn2+, Cu2+, Ni2+, Co2+, Mn2+, Fe3+, Ru3+, VO2+ and UO22+ complexes of 2-hydroxy-5-((4-nitrophenyl) diazenyl) benzylidene)-2-(p-tolyl-amino) acetohydrazide. *Bulletin of the Chemical Society of Ethiopia*, 31(1), 75-91.

[63] Abdou, S., Abd-El Wahed, M. M., Wahba, M. A., Shakdofa, M. M., & Abu-Setta, M. H. *Journal of Chemical, Biological and Physical Sciences.*

[64] Cortijo, M., González-Prieto, R., Herrero, S., Jiménez-Aparicio, R., & Sánchez-Rivera, P. (2013). Ferromagnetic Interactions through Hydrogen Bonds in a OneDimensional NiII Coordination Polymer. *European Journal of Inorganic Chemistry*, 2013(32), 5523-5527.

[65] Cortijo, M., González-Prieto, R., Herrero, S., Jiménez-Aparicio, R., & Sánchez-Rivera, P. (2013). Ferromagnetic Interactions through Hydrogen Bonds in a OneDimensional NiII Coordination Polymer. European *Journal of Inorganic Chemistry*, 2013(32), 5523-5527.

[66] El-Tabl, A. S., Shakdofa, M. M., & El-Seidy, A. (2011). Synthesis, Characterization and ESR Studies of New Copper (II) Complexes of Vicinal Oxime Ligands. *Journal of the Korean Chemical Society*, 55(4), 603-611.

[67] El-Tabl, A. S., El-Kousy, S., Wahba, M. A., & Khalefa, S. M. (2014). Organic Amino Acids Chelates; Preparation, Spectroscopic Characterization and Applications as Foliar Fertilizers. Journal: *Journal of Advances in Chemistry*, 10(2)

[68] . El-Tabl, A. S., Abd-El Wahed, M. M., Wahba, M. A., Shakdofa, M. M., & Gafer, A. (2016). Bimetallic Transition Metal Complexes of 2, 3-Dihydroxy-N', N'4-bis ((2-Hydroxynaphthalen-1-yl) Methylene) Succinohydrazide Ligand as a New Class of Bioactive Compounds; Synthesis, Characterization and Cytotoxic Evaluation. Indian *Journal of Advances in Chemical Science*, 4(1), 114-29.

[69] Emam, S. M., Abdou, S., Ahmed, H. M., & Emad, E. A. (2017). Synthesis, structural characterization, electrochemical and biological studies on divalent metal chelates of a new ligand derived from pharmaceutical preservative, dehydroacetic acid, with 1, 4-diaminobenzene. Arabian *Journal of Chemistry*, 10, S3816-S3825.

[70] . El-Tabl, A. S., El-wahed, M. M. A., & Rezk, A. M. S. M. (2014). Cytotoxic behavior and spectroscopic characterization of metal complexes of

ethylacetoacetate bis (thiosemicarbazone) ligand. Spectrochimica Acta Part A: *Molecular and Biomolecular Spectroscopy*, 117, 772-788

[71] Abdou, S., Abd-El Wahed, M. M., Wahba, M. A., Shakdofa, M. M., & Abu-Setta, M. H. *Journal of Chemical, Biological and Physical Sciences.*

[72] Renfrew, A. K., O'Neill, E. S., Hambley, T. W., & New, E. J. (2017). Harnessing the properties of cobalt coordination complexes for biological application. *Coordination Chemistry Reviews.*

[73] Abdou, S., Abd-El Wahed, M. M., Wahba, M. A., Shakdofa, M. M., & Abu-Setta, M. H. *Journal of Chemical, Biological and Physical Sciences.*.

[74] Sanyal, R., Zhang, X., Chakraborty, P., Mautner, F. A., Zhao, C., & Das, D. (2016). Role of para-substitution in controlling phosphatase activity of dinuclear Ni II complexes of Mannich-base ligands: experimental and DFT studies. *RSC Advances*, 6(77), 73534-73546.